Available online at www.sciencedirect.com
SCIENCE DIRECT®

Journal of Photochemistry and Photobiology A: Chemistry 157 (2003) 223–230

Journal of Photochemistry and Photobiology A:Chemistry
www.elsevier.com/locate/jphotochem

A laser-induced fluorescence study of the $O(^3P) + CF_3I$ and IO + NO reactions Evidence for an association channel for $O + CF_3I$ at low temperatures

T.J. Dillon[1], D.E. Heard*

Department of Chemistry, University of Leeds, Leeds LS2 9JT, UK

Received 12 August 2002; received in revised form 23 September 2002; accepted 23 October 2002

Abstract

The reaction $O(^3P) + CF_3I \xrightarrow{k_1}$ products was monitored by the detection of the product IO using laser-induced fluorescence at 445 nm, with generation of $O(^3P)$ via 248 nm photolysis of O_3 or 193 nm photolysis of N_2O. The temporal evolution of IO as a function of $[CF_3I]$ was used to determine the rate coefficient, k_1, in the temperature range 223–523 K at a variety of pressures. At 223 K, a pressure dependence of k_1 was observed, indicative of an association channel, and for N_2 bath gas the third-order rate coefficient was estimated as $k_{assoc} = (5.5 \pm 2) \times 10^{-31}\ \mathrm{cm^6\ molecule^{-1}\ s^{-1}}$. For $T > 223$ K, k_1 was found to be independent of pressure and was described by the Arrhenius expression:

$$k_1(T) = (9.9 \pm 1.0) \times 10^{-12} \exp\left\{-\frac{(1930 \pm 800)}{RT}\right\}\ \mathrm{cm^3\ molecule^{-1}\ s^{-1}}$$

The rate coefficient for the reaction $IO + NO \xrightarrow{k_2}$ products was measured at $T = 294$ K to be $k_2 = (1.82 \pm 0.1) \times 10^{-11}\ \mathrm{cm^3\ molecule^{-1}\ s^{-1}}$, and independent of pressure.

Keywords: Laser-induced fluorescence; Arrhenius expression; Photolysis; Iodine monoxide; Rate coefficients

1. Introduction

The principal source of iodine atoms in the marine boundary layer (MBL) is the photolysis of biogenic species such as CH_2I_2 and CH_2BrI that have absorption spectra extending into the visible region [1]. Iodine atoms react rapidly with ozone to form the iodine oxide radical, IO. Direct photolysis of IO, and reaction with NO establishes a dynamic equilibrium for the partitioning of reactive iodine in the atmosphere:

$$CH_2I_2 + h\nu\ (\lambda < 380\ \mathrm{nm}) \rightarrow CH_2I + I \tag{3}$$

$$I + O_3 \rightarrow IO + O_2 \tag{4}$$

$$IO + h\nu \rightarrow I + O(^3P) \tag{5}$$

$$IO + NO \rightarrow I + NO_2 \tag{2}$$

IO plays an important role in the gas-phase chemistry of the MBL [2]. Recent observations of IO using differential optical absorption spectroscopy (DOAS) in concentrations of up to 7 ppt at Mace Head, Ireland; Cape Grim, Tasmania and on the coast of Tenerife, in conjunction with periods of low ozone concentrations has provided a fresh impetus to elucidate fully the chemical cycles involving IO [3–5]. The destruction of O_3 can be catalysed by iodine species, for example, as a result of the reaction between IO and HO_2 or the IO self-reaction yielding I atoms [6–10]. Destruction of ozone from iodine mediated chemistry can be similar in magnitude to HO_x chemistry in the MBL [9].

The reaction between $O(^3P)$ and trifluoromethyliodide (CF_3I):

$$O(^3P) + CF_3I \xrightarrow{k_1} IO + CF_3 \tag{1}$$

---

* Corresponding author. Tel.: +44-113-3436471;
fax: +44-113-2336565.
E-mail address: dwayneh@chem.leeds.ac.uk (D.E. Heard).

[1] Present address: Max Planck Institute for Chemistry, Division of Atmospheric Chemistry, Mainz, Germany.

1010-6030/03/$ – see front matter © 2003 Elsevier Science B.V. All rights reserved.
doi:10.1016/S1010-6030(03)00056-X

has been used as a convenient source of IO for laboratory studies. The reaction of $O(^3P)$ with I_2 is often avoided as a source of IO as I_2 is photolabile and undergoes a number of undesirable secondary reactions. Prior to 1995 only two (contradictory) determinations of the rate coefficient k_1 for reaction (1) had been made [11,12]. In 1996, Gilles et al. [13] reported a temperature dependence described by an Arrhenius expression, in agreement with a 1998 study of Hölscher et al. [14]. Gilles et al. reported a branching ratio for the formation of IO, $\Phi_{IO} = 0.83 \pm 0.09$, and speculated that an association channel leading to the formation of CF_3IO or CF_3OI was responsible for up to 10% of the product yield at room temperature [13]. Other possible exothermic product channels are $I + CF_3O$, $IF + CF_2O$ and $I + F + CF_2O$, but little is known about their importance. The value of Φ_{IO} was determined by comparison of the IO yield from the $O(^3P) + CF_3I$ reaction with that from the $O + I_2$ reaction, for which $\Phi_{IO} = 1$ [13]. Despite this suggestion, there was no evidence presented in either study for an association process, such as a pressure dependence for k_1. The value of Φ_{IO} reported by Gilles et al. [13] has been used in the determination of the absorption cross-section for IO, σ_{IO}, by Harwood et al. [15]. For measurement of IO by absorption, either in the laboratory or in field experiments, the value of σ_{IO} is required to convert the measured optical absorption into an absolute concentration. In addition, σ_{IO} is required to calculate the photodissociation lifetime of IO. Hence, atmospheric concentration measurements of IO, or laboratory measurements of the rate of the IO self-reaction (for which [IO] is required) depend critically upon σ_{IO}, and hence, the value of Φ_{IO} from reaction (1) reported by Gilles et al. [13].

In this paper, we report the rate coefficient k_1 for the $O + CF_3I$ reaction as a function of temperature and pressure, and present evidence for the existence of an association channel for this reaction, but only at the lowest temperature studied (223 K). The implications of this result in terms of the yield of IO for this reaction, Φ_{IO}, are discussed. We report also a measurement of the rate coefficient k_2 for the IO + NO reaction (2) at room temperature.

2. Experimental

Flash-photolysis coupled with laser-induced fluorescence (LIF) detection of IO was used to investigate the kinetics of reactions (1) and (2). The experimental set-up has been described before [16] and so a brief description is given here except for details pertaining to the generation and detection of IO. An excimer laser (Lambda Physik MINEx) operating at 193 nm (ArF) or 248 nm (KrF) (5–15 mJ cm^{-2} in a 15 ns pulse) was used to initiate the production of IO. The second harmonic of a YAG laser at 532 nm (Quanta-Ray 300) was used to pump a dye laser (Spectra Physics PDL-3) operating at 765 nm (Styril-8 dye, Radiant Dyes) to generate a 10 mJ, 10 ns laser pulse that was sum-frequency mixed in a KDP crystal with the depleted 1064 nm YAG fundamental to generate radiation at 445 nm (200 μJ/15 ns pulse). The phase matching angle was controlled using an autotracking system (Spectra Physics, WEX). The radiation at 445 nm was used to excite the IO radical via excitation of the $A^2\Pi_{3/2} \leftarrow X^2\Pi_{3/2}$ (2, 0) band, using a glass cut-off filter (Schott Glass, $\lambda > 495$ nm) to transmit fluorescence from IO whilst discriminating against scattered laser light. The LIF was collected using a photomultiplier tube (PMT) with the axes of the two laser beams and the fluorescence collection axis mutually perpendicular to minimise the collection of scattered laser light. The PMT signal was amplified using a fast pre-amplifier (SRS-445) and captured by a boxcar integrator (SRS-250) whose output was digitised and recorded by a personal computer together with the output of two photodiodes that monitored the relative energies of the pump- and probe-laser pulses. The excited state of IO is highly pre-dissociative, with the 200 ps lifetime of $A^2\Pi_{3/2} v' = 2$ [17] being much less than the ∼15 ns laser pulse, and hence, the integration gate of the boxcar was set directly over the temporal profile of the probe-laser pulse. Due to the short lifetime of the excited state, the LIF signal from IO was not significantly quenched even when air was used as the bath gas. The temporal evolution of IO following the photolysis laser was determined by incrementally changing the delay between the firing of the photolysis- and probe-lasers and recording the LIF signal.

The reaction cell (a six-way cross) and surrounding cooling box were manufactured from a single (40 cm × 40 cm × 40 cm) block of black PTFE. Temperatures in the range $223\,K < T < 294\,K$ were regulated by a cooling probe (LabPlant RP-100-CD) and a curtain of N_2 was flowed over the cell windows to prevent icing. For experiments above 300 K, a stainless-steel reaction cell of dimensions 15 cm × 15 cm × 15 cm was used, with temperature control achieved by a series of three cartridge heaters coupled to a calibrated thermocouple situated at the centre of the cell. A glass vacuum line was used for preparation, storage and supply of the reagents used in these experiments. The gases, together with the suppliers' stated purities were as follows: NO, Air Products, Technical Grade 99.9%; N_2O, BDH, Research Grade 99.5%; CF_3I, Fluorochem, 99%; N_2 and He, Air Products, Premier Grade 99.999%; Synthetic Air, BOC, BTCA 178. N_2O and NO were purified via trap-to-trap distillation, whilst CF_3I was degassed by repeated freeze–pump–thaw cycles. These reagents were then diluted in He and stored in one of six 10 dm^3 glass bulbs. All other gases were used as supplied. The reagents were combined with a much larger flow of N_2 or synthetic air and mixed in a steel manifold prior to entering the reaction cell through a 2 m length of PTFE tubing. All gas flows were regulated by mass flow controllers (Tylan General FC280).

The volumetric flow rate (3000–7500 sccm) and the laser pulse-repetition-frequency (5 Hz) were such that there was no accumulation of products in the photolysis cell. Laser excitation spectra of the $A^2\Pi_{3/2} \leftarrow X^2\Pi_{3/2}$ (2, 0) band of IO between 445 and 446 nm were recorded with a fixed time delay between the two laser pulses ($\Delta t = 1$ ms), and comparison made with experimental and simulated spectra from the literature to ensure that the LIF signal originated solely from IO. In the majority of experiments, the photolysis of N_2O at 193 nm was used to generate $O(^1D)$ atoms, that were collisionally relaxed on a short timescale ($t < 1\,\mu s$) to ground-state $O(^3P)$ atoms by the bath gas (N_2 or air). The photolysis of O_3 at 248 nm was used as an alternative source of $O(^1D)/O(^3P)$ (with subsequent relaxation of $O(^1D)$ to $O(^3P)$) in one determination of the rate coefficient of reaction (1). Low concentrations of O_3 ($<1 \times 10^{13}$ molecule cm^{-3}) were generated by passing the main flow of synthetic air over a mercury pen-lamp (Oriel, 6035/6060), and quantified by measuring the attenuation of the 248 nm laser output over a path length of 40 cm. IO was formed by the rapid reaction of $O(^3P)$ with CF_3I (or CH_3I as used in one determination of the rate coefficient for reaction (2)):

$$N_2O + h\nu\,(193\,\mathrm{nm}) \rightarrow O(^1D) + N_2 \quad (6)$$

$$O(^1D) + N_2 \rightarrow O(^3P) + N_2 \quad (7)$$

$$O(^3P) + CF_3I \rightarrow IO + CF_3 \quad (1)$$

At the concentrations and laser fluences used in this work the concentration of IO generated by this scheme was $\sim 10^{11}$ molecule cm^{-3}, considerably lower than used in some previous studies. At 295 K and 760 Torr, the rate constant for the IO self-reaction is 8.2×10^{-11} cm^3 molecule^{-1} s^{-1} [18], and thus, the half-life of IO by self-reaction is ~0.1 s and can be ignored as a loss for IO on the timescales of these experiments. IO was also generated using the reaction of $O(^3P)$ with either I_2 or CH_3I, with $O(^3P)$ generated from NO_2 photolysis at 193 or 308 nm, or from a microwave discharge of O_2. For kinetic experiments, IO was detected after excitation at the (2, 0) bandhead at 445.054 nm.

3. Results and discussion

3.1. The reaction $O(^3P) + CF_3I \rightarrow IO$ (+ other products)

Fig. 1 shows the temporal evolution of IO following the formation of $O(^3P)$ in the presence of an excess of CF_3I at 294 K, using N_2 as the buffer gas, and N_2O as the O atom precursor. The LIF signal was recorded at 100 values of the delay between the photolysis and probe-laser pulses, and the signal for each time delay was normalised for the variation in laser pulse energies. A series of experiments was performed at various $[CF_3I]$ in the range 1.4 – 13.0 $\times$ 10^{14} molecule cm^{-3}. The data were analysed by fitting a two-parameter single exponential growth function S_{IO} to the temporal profile of the IO LIF signal:

$$S_{IO} = A\{1 - \exp(-k't)\} \quad (E1)$$

where k' is the pseudo-first-order rate coefficient for the production of IO, given by $k' = k_1[CF_3I]$, and A is a scaling factor. Experiments using considerably longer delay times than shown in Fig. 1 determined that in the absence of any other reagents the decay of IO occurred on a timescale of approximately 20 ms, much longer than the risetime, and ignoring the slow decay of IO made no difference to the value of k' retrieved from the fit of (E1) to the data. Fig. 2 shows a plot of k' against $[CF_3I]$, the gradient of which yields the bimolecular rate coefficient for the reaction $O(^3P) + CF_3I$ at 294 K, $k_1 = (4.6 \pm 0.3) \times 10^{-12}$ cm^3 molecule^{-1} s^{-1} (2σ), in excellent agreement with the result obtained by Gilles et al. (see Table 2). Implicit in this analysis is the assumption that there are no processes other than reaction (1) that generate IO ($v = 0$). The value of k_1 was also measured at 294 K using 248 nm photolysis of O_3 as the O atom source in the presence of CF_3I using synthetic air as the buffer gas. A

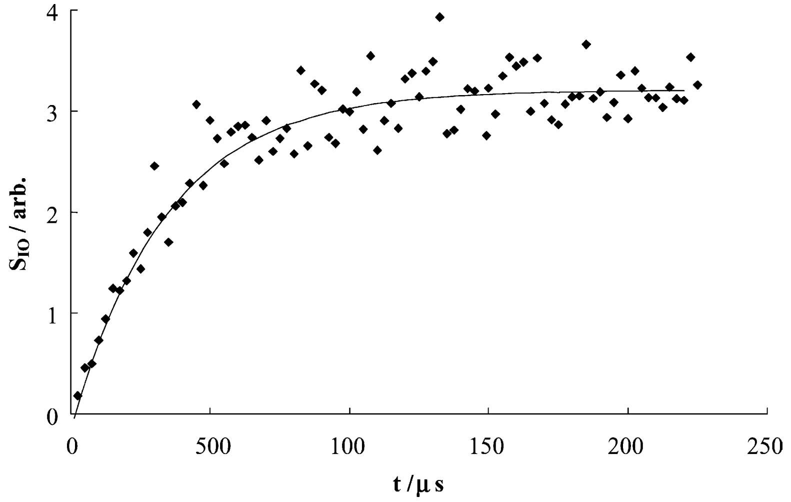

Fig. 1. Exponential growth of the IO laser-induced fluorescence signal, S_{IO}, following production via the $O(^3P) + CF_3I$ reaction. The solid line is a non-linear least squares fit of Eq. (E1) to the data yielding $k' = 2921 \pm 221$ s^{-1}. The experimental conditions used were $T = 294$ K, $[CF_3I] = 4.3 \times 10^{14}$ and $[N_2O] = 1.9 \times 10^{15}$ molecule cm^{-3}, total pressure 18.0 Torr in N_2. Each of the 100 data points has been averaged over 10 laser shots.

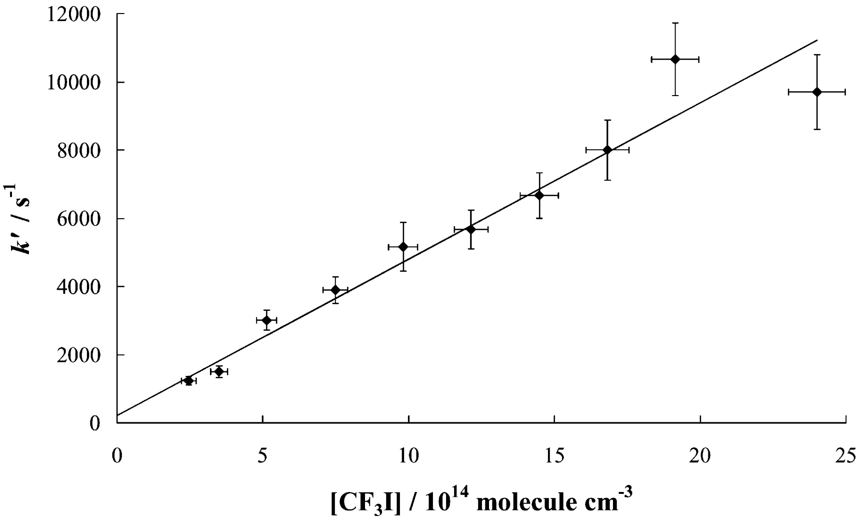

Fig. 2. A plot of k' vs. [CF_3I] at 294 K. The line is the weighted least squares fit to the data and yields the rate coefficient $k_1 = (4.59 \pm 0.3) \times 10^{-12}$ cm^3 molecule^{-1} s^{-1}. The experimental conditions used were [N_2O] = 1.9×10^{15} molecule cm^{-3} and total pressure 25 Torr (N_2).

value of $k_1 = (4.4 \pm 0.5) \times 10^{-12}$ cm^3 molecule^{-1} s^{-1} (2σ) was obtained, in excellent agreement with the value using N_2O as the precursor. When using O_3 as the precursor, the plot of k' against [CF_3I] was characterised by a significant intercept due to the competing $O(^3P) + O_2 + M \rightarrow O_3 + M$ process. This observation, together with the fact that some I atoms are formed at 248 nm as a result of CF_3I photolysis ($\sigma_{248} = 2.5 \times 10^{-19}$ cm^2), potentially complicating the study of IO reactions, resulted in the use of 193 nm photolysis of N_2O as the source of IO in all further experiments. However, the consistent value of k_1 obtained using the two IO sources gives confidence that there are no secondary reactions that significantly complicate the kinetic analysis. Experiments were repeated at five different temperatures over the range 223 K $< T <$ 523 K, and the values of k_1 obtained are listed in Table 1, and plotted in Arrhenius form, together with those obtained by Gilles et al. [13] and Hölscher et al. [14] in Fig. 3.

A comparison of the results from this work with all the previous studies of the $O(^3P) + CF_3I$ reaction is given in Table 2. The room temperature data are in very good agreement with the result of Gilles et al. [13], and the activation energy of $E_a = 1930 \pm 800$ J mol^{-1} agrees well with the values reported by Gilles et al. [13] and Hölscher et al. [14], although the range of temperatures studied is wider in this work. The less than unity branching ratio for IO from reaction (1) has been postulated as due to an association channel leading to the formation of an [O–CF_3I] adduct [13], but none of the previous studies [11–14,19] report a pressure dependence of the reaction. Similarly, we do not see a pressure dependence of the rate coefficient k_1 for any experiments (20 Torr $< p <$ 200 Torr) undertaken at ambient temperature. However, at the lowest temperature studied (223 K), there was a ca. 40% reduction in the intensity of the IO LIF signal compared to that at 294 K, in contrast to the study by Gilles et al. who observed no reduction in fluorescence intensity down to $T = 254$ K [13]. Recently, Bloss et al. reported a pressure dependence of the IO yield at 220 K, observing ca. 20% reduction in yield between 100 and 760 Torr [18]. No pressure dependence of the yield was observed at 295 K [18]. At 223 K, we have observed a weak pressure dependence of k_1, as shown in Fig. 4, indicative of an association channel in competition with the channel generating IO. The two channel reaction can be expressed by the scheme:

$$O + CF_3I \rightarrow [CF_3IO]^* \rightarrow IO + CF_3, \quad \Delta_r H^\circ_{298} = -21\ \mathrm{kJ\,mol^{-1}} \tag{1a}$$

$$O + CF_3I \rightarrow [CF_3IO]^* \xrightarrow{N_2} CF_3IO \text{ or } CF_3OI \tag{1b}$$

The absence of a pressure dependence at 298 K suggests the initially formed complex is weakly bound, but there are insufficient data to estimate the enthalpy of formation of the O–CF_3I adduct. Assuming the reaction is at the low-pressure limit, the intercept from the linear fit to the data of Fig. 4 yields $k_{1a} = (3.5 \pm 0.4) \times 10^{-12}$ cm^3 molecule^{-1} s^{-1}, the rate coefficient for the non-association channels (principally IO + CF_3 formation) at 223 K. The gradient of the fit shown in Fig. 4 gives the termolecular

Table 1
Temperature dependence of k_1 for the reaction between $O(^3P)$ and CF_3I

T (K)	k_1 ($\times 10^{-12}$ cm^3 molecule^{-1} s^{-1})
223	3.67 ± 0.4
263	3.97 ± 0.3
294[a]	4.40 ± 0.5
294	4.59 ± 0.3
423	5.51 ± 0.2
523	6.72 ± 0.8

[a] Photolysis of O_3 used as source of O atoms.

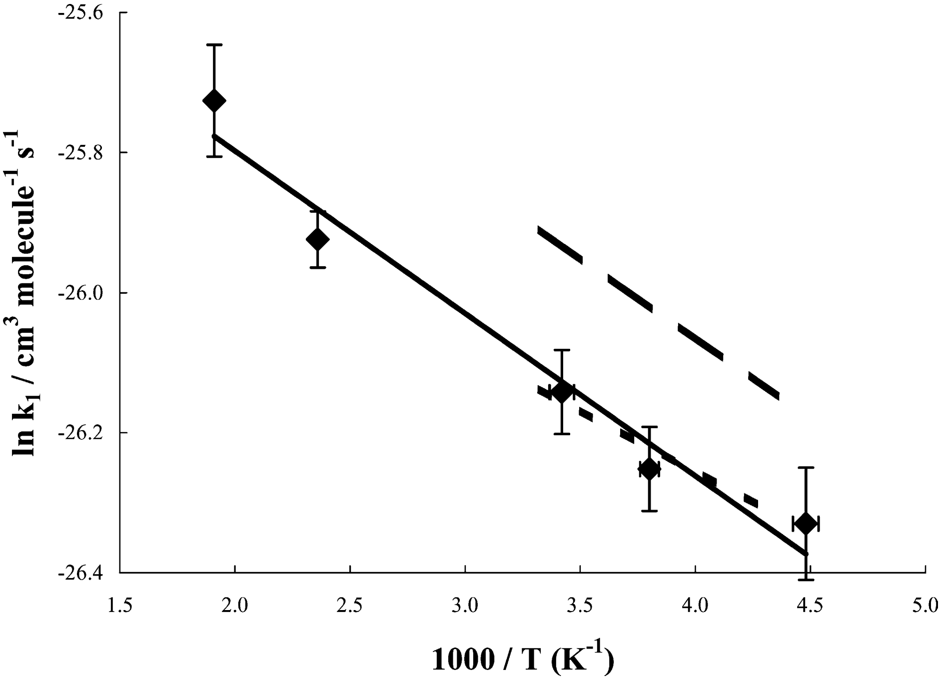

Fig. 3. Arrhenius plot showing the temperature dependence of k_1 with $[N_2]$ held constant at 8.0×10^{17} molecule cm^{-3}. The diamonds with error bars are the experimental data and the solid line is a linear least squares fit to the data yielding $E_a = 1930\pm800$ J mol^{-1} and $A = (9.9\pm1.0)\times10^{-12}$ cm^3 molecule^{-1} s^{-1}. The short-dashed and long-dashed lines show the Arrhenius behaviour observed by Gilles et al. [13] and Hölscher et al. [14], respectively.

Table 2
Arrhenius parameters for the reaction $O(^3P) + CF_3I \rightarrow$ products

	Pressure (Torr)	k_1 (298 K) (cm^3 molecule^{-1} s^{-1})	A (cm^3 molecule^{-1} s^{-1})	E_a (J mol^{-1})
This work	25 (N_2)	4.6 ± 0.3	9.9 ± 1.0	1931 ± 800
Gilles et al. [13]	50 (N_2)	4.4 ± 0.4	7.9 ± 0.8	1455 ± 335
Hölscher et al. [14]	51 (N_2)	5.3 ± 0.25	13.0 ± 4.9	2212 ± 708
Watson et al. [11]	10 (N_2)	6.5 ± 1.5	–	–
Addison et al. [12]	6.0 (N_2)	11 ± 3	–	–
Atkinson et al. [19]	9.4, 30.1 (Ar)	5.8 ± 1.5[a]	–	–

[a] 295 K.

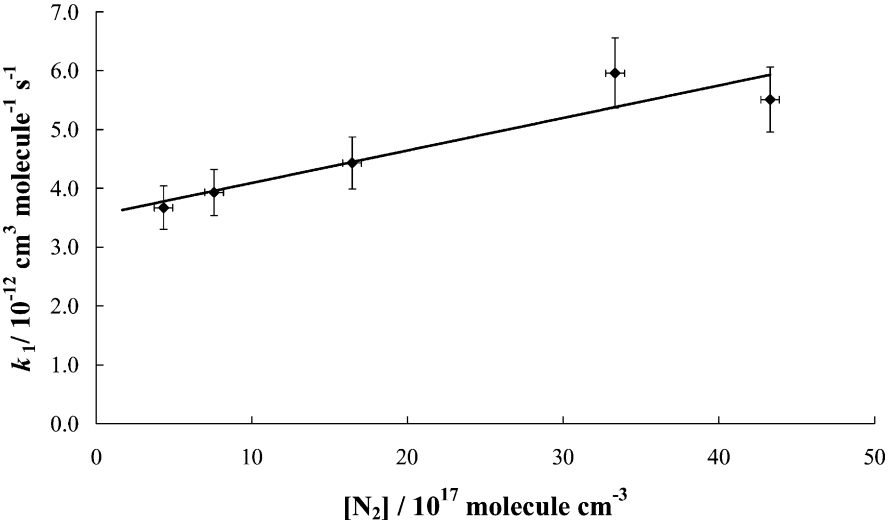

Fig. 4. Pressure dependence of k_1 at 223 K. The range of $[N_2]$ on the x-axis is equivalent to 0–100 Torr at 223 K. The gradient gives a third-order rate coefficient of $k_{assoc} = (5.5\pm1.9)\times10^{-31}$ cm^6 molecule^{-2} s^{-1} and the intercept yields a value of k_1 at zero pressure of $(3.5\pm0.4)\times10^{-12}$ cm^3 molecule^{-1} s^{-1}.

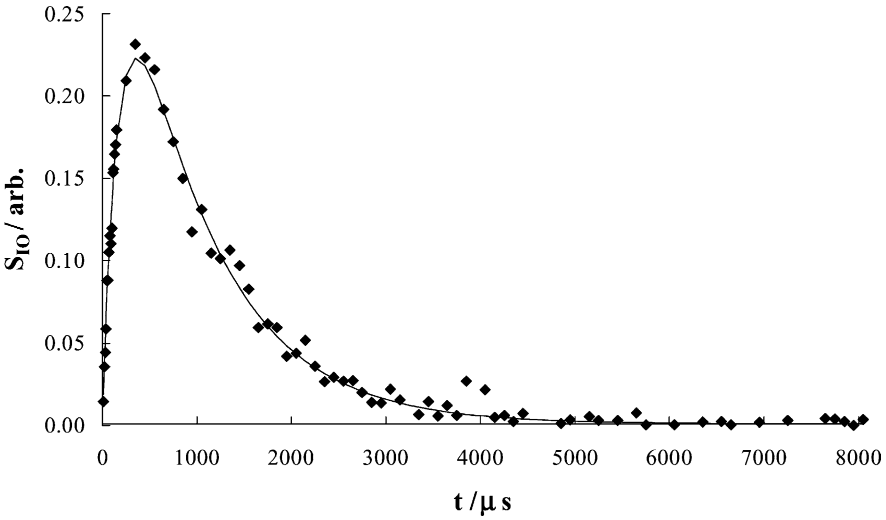

Fig. 5. Temporal evolution of IO following production in the presence of NO together with a non-linear least squares fit of the bi-exponential expression given by Eq. (E3). The experimental conditions are $T = 294\,K$; $p = 64\,Torr$ (N_2); $[CH_3I] = 1.3 \times 10^{15}$, $[N_2O] = 4.5 \times 10^{14}$ and $[NO] = 2.67 \times 10^{14}$ molecule cm^{-3}. The fit yields a decay constant $k' = 1107\,s^{-1}$.

rate coefficient for the association reaction as $k_{assoc} = (5.5 \pm 1.9) \times 10^{-31}\,cm^6\,molecule^{-2}\,s^{-1}$ for $M = N_2$. However, the range of pressures at which $k_1 = k_{1a} + k_{1b}$ was determined is clearly not wide enough to establish whether the reaction is at the low-pressure limit or not, and hence, no attempt is made to estimate $\Phi_{IO} = k_{1a}/k_1$ from these results.

The other thermodynamically favourable channels of reaction (1) (ignoring the production of spin–orbit excited I atoms) are [13,14]:

$$O(^3P) + CF_3I \rightarrow I + CF_3O, \quad \Delta_r H^\circ_{298} = -209\,kJ\,mol \tag{1c}$$

$$O(^3P) + CF_3I \rightarrow IF + CF_2O, \quad \Delta_r H^\circ_{298} = -362\,kJ\,mol \tag{1d}$$

$$O(^3P) + CF_3I \rightarrow I + F + CF_2O, \quad \Delta_r H^\circ_{298} = -84\,kJ\,mol \tag{1e}$$

and although IF can be observed with good sensitivity using cavity ring-down spectroscopy [17], it was not observed as a product of this reaction [19]. Therefore, at room temperature, it would appear that the non-IO forming product channel is most likely to be that forming I atoms (1c and 1e), although Gilles et al. reported a yield of CF_3O of <0.01 [13]. Further studies with direct detection of the products are clearly necessary to quantify the branching ratios of product channels other than the channel forming IO (1a).

3.2. *The reaction IO + NO → I + NO$_2$*

When NO is added to the reaction mixture the IO radicals generated by the reaction between $O(^3P)$ and CF_3I (reaction (1)) are removed by reaction with NO (reaction (2)). If other sources and sinks or IO are neglected, and assuming $[CF_3I] \gg [O(^3P)]$ and $[NO] \gg [IO]$, a kinetic analysis yields the following bi-exponential expression for the temporal profile of IO:

$$[IO](t) = \frac{k_1[O(^3P)]_0}{k_2[NO] - k_1[CF_3I]_0}(\exp(-k_1[CF_3I]t) - \exp(-k_2[NO]t)) \tag{E2}$$

For a given $[CF_3I]$ and $[N_2O]$ (and hence $[O(^3P)]_0$), the temporal profile of the IO fluorescence signal, S_{IO}, was recorded for a range of NO concentrations, under pseudo-first-order conditions of $[NO] \gg [IO]$, and Fig. 5 shows a typical profile of S_{IO} for a given [NO], together with a non-linear least squares fit to S_{IO} using the function:

$$S_{IO} = A\{\exp(-Bt) - \exp(-Ct)\} \tag{E3}$$

The data are described well by Eq. (E3), and the parameters A, B and C can be related to the rate coefficients k_1 and k_2 via the expressions:

$$B = k_1 \times [CF_3I]_0$$

$$C = k_2 \times [NO]$$

$$A = \frac{k_1[O(^3P)]_0}{C - B}$$

It should be noted that under the experimental conditions used, $B > C$ and the decay of IO is associated with parameter C. The above analysis assumes that the rate of loss of IO by other reactions or by diffusion is negligible compared to loss by reaction with NO. The values of C obtained following the analysis of S_{IO} at various [NO] are plotted in Fig. 6 for 294 K. A weighted linear-least squares fit yields the bimolecular rate coefficient k_2 for the IO + NO reaction as the gradient. The weighting for each point at a given [NO]

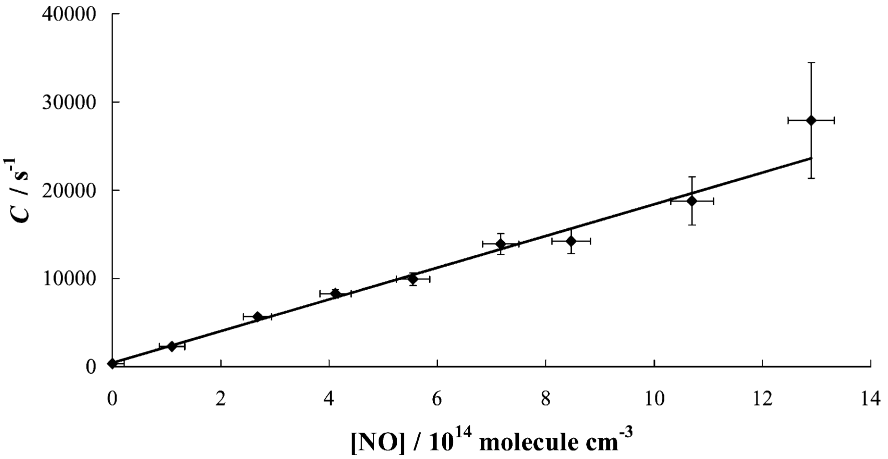

Fig. 6. A plot of the parameter C from Eq. (E3) vs. [NO]. The gradient yields $k_2 = (1.80 \pm 0.15) \times 10^{-11}$ cm^3 $molecule^{-1}$ s^{-1}. The experimental conditions are given in Fig. 5.

was determined from the statistical error in the fitting of the bi-exponential expression to the data, added in quadrature to the ca. 5% systematic error in the measurement of [NO]. The absence of a significant intercept (~450 s^{-1}) confirms that reaction with NO is the dominant loss process for IO. Table 3 lists the values of k_2 obtained via this analysis for a variety of initial N_2O and CF_3I concentrations at 294 K. It can be seen that within the uncertainty of the experiment the value of k_2 is independent of the initial concentration of CF_3I and N_2O, and the total pressure. A weighted average of k_2 using all the conditions employed gives $k_2 = (1.82 \pm 0.1) \times 10^{-11}$ cm^3 $molecule^{-1}$ s^{-1}, in good agreement with previously reported data.

Preliminary attempts to study this reaction using He as the bath gas, with a small amount of N_2 added to facilitate the quenching of $O(^1D)$ to $O(^3P)$ following photolysis, yielded values of k_2 that were dependent upon $[N_2]$. Daykin and Wine reported a similar finding [20] and ascribed the behaviour to the production of vibrationally excited IO from reactions of $O(^3P)$ or $O(^1D)$ with the precursor followed by vibrational relaxation of $v'' > 0$ to the vibrational ground state $v'' = 0$ that is probed by the laser. The production of the laser-probed level, and hence, the temporal profile of the IO LIF signal, is therefore not only controlled by reaction (1) but also by vibrational relaxation of IO. Attempts to detect IO $v'' = 1$ by LIF through laser excitation of the (2, 1) band at 459.1 nm were unsuccessful. However, Turnipseed et al. [21] reported that the LIF signal from IO when exciting LIF via the (2, 1) band was an order of magnitude weaker than for excitation in the (2, 0) band, leaving open the possibility that there was indeed IO $v'' > 0$ generated but that a lack of sensitivity in our experiment (due partly to low laser fluences at 459.1 nm) precluded its detection. All the experiments for which rate coefficients are reported in this work employed N_2 or synthetic air as the bath gas to ensure the rapid relaxation of any vibrationally excited IO. As shown in Table 3, the value of k_2 was independent of the total pressure, suggesting that although the channel to form IONO is thermodynamically favourable, the decomposition of the initially formed IONO* complex to form I + NO_2 is much faster than collisional stabilisation.

Table 3
Rate coefficients k_2 at room temperature for the reaction IO + NO → I + NO_2

	$[N_2O]$[a]	$[CF_3I]$[a]	[NO][a]	p (Torr)	k_2 ($\times 10^{-11}$ cm^3 $molecule^{-1}$ s^{-1})
This work	20	70	0–50	66	1.93 ± 0.15
This work	30	130	0–50	130	1.74 ± 0.13
This work[b]	45	130[b]	0–130	64	1.80 ± 0.15
This work (weighted average)				64–130	1.82 ± 0.1
Atkinson et al. [19]				9–30	1.90 ± 0.5
Daykin and Wine [20]				40–200	2.08 ± 0.2
Turnipseed et al. [21]				5–100	1.90 ± 0.3
Inoue et al. [22]				0.4–0.8	2.80 ± 0.2
Ray and Watson [23]				2	1.67 ± 0.162
Hölscher and Zellner [24]				10–99	1.68 ± 0.11
Knight and Crowley [25]				1–2	2.05 ± 0.57

[a] Units of 10^{13} molecule cm^{-3}.
[b] CH_3I used as I atom donor.

4. Conclusions

Although CF_3I plays no significant atmospheric role, its reaction with $O(^3P)$ is used extensively as a laboratory source of the IO radical. The yield of IO from this reaction is crucial in the determination of the absolute IO concentration that is used to measure the absorption cross-section and the rate coefficient of the IO self-reaction. We have used a frequency-mixing technique to generate laser radiation at 445 nm to detect IO via laser-induced fluorescence spectroscopy via the A–X (2, 0) transition. The temperature dependence of the rate coefficient for the $O + CF_3I$ reaction that yields IO was determined between 223 and 523 K and was found to be in good agreement with recent measurements. We observed no pressure dependence of the rate coefficient at room temperature, inconsistent with the previous suggestion that the less than unity branching ratio for IO from this reaction may be due to a CF_3IO or CF_3OI complex forming channel. Instead it would appear that the initially formed vibrationally excited complex is not stabilised but decomposes to form other products in addition to IO. However, we did observe a weak pressure dependence for this reaction at 223 K, suggesting the presence of the complex forming channel under these conditions. Further studies of the $O + CF_3I$ reaction with direct product detection are necessary to quantify the product branching ratios for this reaction. The reaction between IO and NO was studied at room temperature and the rate coefficient measured was found to be in good agreement with previous studies.

Acknowledgements

We are grateful to the NERC for the provision of a postgraduate studentship (TJD) and to the Royal Society for the provision of a University Research Fellowship (DEH) and some equipment funding. We are also grateful to the referees for insightful comments.

References

[1] L.J. Carpenter, W.T. Sturges, S.A. Penkett, P.S. Liss, B. Alicke, K. Hebestreit, U. Platt, J. Geophys. Res. A 104 (1999) 1679.

[2] R.P. Wayne, G. Poulet, P. Biggs, J.P. Burrows, R.A. Cox, P.J. Crutzen, G. Hayman, M.E. Jenkin, G. LeBras, G.K. Moortgat, U. Platt, R.N. Schindler, Atmos. Environ. 29 (1995) 2677.

[3] B.J. Allan, G. McFiggans, J.M.C. Plane, H. Coe, J. Geophys. Res. A 105 (2000) 14363.

[4] B. Alicke, K. Heibestreit, J. Stutz, U. Platt, Nature 397 (1999) 572.

[5] B.J. Allan, J.M.C. Plane, G. McFiggans, Geophys. Res. Lett. 28 (2001) 1945.

[6] P.O. Wennberg, J.W. Brualt, T.F. Hanisco, R.J. Salawitch, G.H. Mount, J. Geophys. Res. A 102 (1997) 8887.

[7] R. Vogt, R. Sander, R. von Glasow, P.J. Crutzen, J. Atmos. Chem. 32 (1999) 375.

[8] S. Solomon, R.R. Garcia, A.R. Ravishankara, J. Geophys. Res. A 99 (1994) 20491.

[9] G. McFiggans, J.M.C. Plane, B.J. Allan, L.J. Carpenter, H. Coe, C. O'Dowd, J. Geophys. Res. A 105 (2000) 14371.

[10] R.A. Cox, W.J. Bloss, R.L. Jones, D.M. Rowley, Geophys. Res. Lett. 26 (1999) 1857.

[11] T.A. Watson, M. Addison, C. Wittig, Chem. Phys. 78 (1983) 57.

[12] M.C. Addison, R.J. Donovan, J. Garraway, J. Chem. Soc. Faraday Disc. 67 (1980) 286.

[13] M.K. Gilles, A.A. Turnipseed, R.K. Talukdar, Y. Rudich, P.W. Villalta, L.G. Huey, J.B. Burkholder, A.R. Ravishankara, J. Phys. Chem. 100 (1996) 14005.

[14] D. Hölscher, C. Fockenberg, R. Zellner, Ber. Bunsenges. Phys. Chem. 102 (1998) 716.

[15] M.H. Harwood, J.B. Burkholder, M. Hunter, R.W. Fox, A.R. Ravishankara, J. Phys. Chem. 101 (1997) 853.

[16] D.E. Heard, D.A. Henderson, Phys. Chem. Chem. Phys. 2 (2000) 67.

[17] S.M. Newman, W.H. Howie, I.C. Lane, M.R. Upson, A.J. Orr-Ewing, J. Chem. Soc. Faraday Trans. 94 (1998) 2681.

[18] W.J. Bloss, D.M. Rowley, R.A. Cox, R.L. Jones, J. Phys. Chem. A 105 (2001) 7840.

[19] D.B. Atkinson, J.W. Hudgens, A.J. Orr-Ewing, J. Phys. Chem. A 103 (1999) 6173.

[20] E.P. Daykin, P.H. Wine, J. Phys. Chem. 94 (1990) 4528.

[21] A.A. Turnipseed, M.K. Gilles, J.B. Burkholder, A.R. Ravishankara, Chem. Phys. Lett. 242 (1995) 427.

[22] G. Inoue, M. Suzuki, N. Washida, J. Chem. Phys. 79 (1983) 4730.

[23] G.W. Ray, R.T. Watson, J. Phys. Chem. 85 (1981) 2955.

[24] D. Hölscher, R. Zellner, Phys. Chem. Chem. Phys. 4 (2002) 1839.

[25] G.P. Knight, J.N. Crowley, Phys. Chem. Chem. Phys. 3 (2001) 393.